Behavioral/Systems/Cognitive

A Simple Account of Cyclopean Edge Responses in Macaque V2

Christine E. Bredfeldt and Bruce G. Cumming
Laboratory of Sensorimotor Research, National Eye Institute, Bethesda, Maryland 20892

It has been shown recently that neurons in V2 respond selectively to the edges of figures defined only by disparity (cyclopean edges). These responses are orientation selective, often preferring similar orientations for cyclopean and luminance contours, suggesting that they may support a cue-invariant representation of contours. Here, we investigate the extent to which processing of purely local visual information (in the vicinity of the receptive field) might explain such results, using the most impoverished stimulus possible containing a cyclopean edge (a circular patch of random dots divided into two regions by a single edge). Many V2 cells responded better to the cyclopean edge than to uniform disparities, and most of these were at least broadly selective for the orientation of the cyclopean edge. Two characteristics argue against a cue-invariant contour representation: (1) the cyclopean edge response was frequently abolished by small changes to the component disparities; and (2) although V2 cells frequently responded to both signs of a cyclopean edge (defined by which side of the edge is in front), they did so at different edge locations. These characteristics are consistent with a simple feedforward scheme in which V2 neurons receive inputs from several V1 subunits with different disparity selectivity. We also found a correlation between the preferred orientations for cyclopean edges and contrast stimuli, suggesting that this feedforward wiring is not random. These characteristics suggest that V2 responses to cyclopean edges may be useful in supporting a cue-invariant contour representation higher in the visual pathway.

Key words: **vision; binocular; macaque; V2; contour; disparity**

Introduction

Recent studies have suggested that V2 may play a role in generating visual responses to relatively complex stimuli such as motion-defined borders (Marcar et al., 2000), illusory contours (von der Heydt et al., 1984; Leventhal et al., 1998), angles (Ito and Komatsu, 2004), and oriented borders defined only by disparity ("cyclopean edges") (von der Heydt et al., 2000; Qiu and von der Heydt, 2005). These results, combined with the observation that some V2 cells signal border ownership of luminance contours, have led to the suggestion that V2 may be the first step in representing figure-ground segregation (Zhou et al., 2000; Qiu and von der Heydt, 2005).

However, a simpler explanation for these complex responses is that they reflect the feedforward convergence of diverse inputs from V1, in which the inputs differ in orientation (Ito and Komatsu, 2004), direction, or disparity preference. Here, we examine the possibility that this simple scheme might account for the responses to cyclopean edges. Previous reports of cyclopean edge selectivity have used gestalt figures defined by disparity to probe V2 neurons (von der Heydt et al., 2000; Qiu and von der Heydt, 2005), making it difficult to determine whether the response is determined only by the cyclopean edge in the receptive field (a possibility recognized in these reports), or results from long-range interactions reflecting the presence of a gestalt figure. A distinctive feature of simple feedforward explanations is that they predict responses to cyclopean contours even in impoverished stimuli that do not contain a clearly defined figure or ground. We therefore studied responses to the orientation and position of a cyclopean edge using the most impoverished stimulus that can still define the contour: a circular patch of random dots divided in two by a single cyclopean edge. This stimulus contains no perceptual figure: binocularly it appears as two floating disc segments (at different depths), whereas monocularly the stimulus appears as a uniform cloud of random dots.

A second important property of simple convergence models is that they have limited scope to represent boundaries independently of the cues that define them (cue invariance). If cyclopean edge responses identify figure-ground borders, they should show cue invariance, perhaps comparable to that shown by V1 complex cells for luminance. Cyclopean edge responses should, for example, be similar regardless of the disparities used to define the boundary. Conversely, signals generated primarily through feedforward convergence may be sensitive to attributes such as position and disparity, reflecting the tuning of the input subunits. We examine this distinction here by measuring responses to a range of edge orientations, edge locations, and disparities. This generates a data set that is rich enough to provide stringent tests for the idea that these responses are generated by a simple feedforward mechanism. Thus, examining such responses from V2 neurons

Received Dec. 13, 2005; revised May 11, 2006; accepted June 4, 2006.

This work was supported by the Intramural Research Program of the National Institutes of Health–National Eye Institute. We thank Jenny Read for helpful discussions and mathematical support.

Correspondence should be addressed to Dr. Christine E. Bredfeldt, Laboratory of Sensorimotor Research, National Eye Institute, 49 Convent Drive, 2A50, Bethesda, MD 20892. E-mail: cb@nei.nih.gov.

DOI:10.1523/JNEUROSCI.5308-05.2006

Copyright © 2006 Society for Neuroscience 0270-6474/06/267581-16$15.00/0

allows us to quantify the role that simple local processes play in generating responses that appear to code for complex stimulus attributes.

Materials and Methods

We recorded extracellularly from isolated V2 neurons in the lunate sulcus of two awake, fixating rhesus macaque monkeys. Details of the experimental protocol were described previously (Read and Cumming, 2003). All protocols were approved by the Institute Animal Care and Use Committee and complied with Public Health Service policy on the humane care and use of laboratory animals.

In brief, monkeys perched in a primate chair with their heads immobilized. A digitally controlled microdrive was used to lower electrodes (glass-coated PtIr; FHC, Bowdoin, ME) through the dura into V1. Spikes were isolated based on the height and width of the electrical waveforms. All electrical activity crossing a manually set voltage threshold was saved for off-line analysis with a precision of 0.1 ms. The positions of both eyes were recorded with scleral search coils (implanted under general anesthesia). Stimuli were presented on two Eizo Flexscan F980 monitors (96 Hz frame rate; mean luminance, 41.1 cd/m^2; contrast, 99%) viewed through a Wheatstone stereoscope.

As soon as the electrode penetrated the dura, multiunit V1 receptive fields were manually mapped using bars and gratings. Once the approximate size and location of the V1 receptive fields were assessed, the electrode was lowered slowly through V1. Changes in spontaneous firing rate, ocularity, and orientation selectivity were noted to provide landmarks on the way through V1. The end of V1 was marked by a significant reduction in electrical activity as the electrode entered the white matter. Resumption of electrical activity signaled the presence of the electrode in V2. Entrance into V2 was confirmed by changes in the size and location of the receptive fields. Receptive fields were located between 1 and 10° from the fovea, and ranged from 1 to 4° in diameter (determined manually). See Figure 1*a* for a schematic of the experimental setup.

For all experiments, trials lasted ~2 s, during which the monkey was required to maintain fixation within a 0.8° window. If the monkey successfully maintained fixation throughout the trial, he received a water reward. Each trial consisted of four 420 ms stimulus presentations, separated by 100 ms blank periods. If the monkey broke fixation before the end of the trial, the successfully completed stimulus presentations were saved, but the monkey did not receive a reward. Responses were measured as the mean spike rate over the entire stimulus presentation, beginning 50 ms after stimulus onset.

V2 receptive fields were initially mapped manually using both bars and gratings to determine their approximate location, size, orientation, and ocularity. Additionally, many cells (including all example cells) had their receptive fields quantitatively mapped using the stimuli described by Read and Cumming (2003). We then performed systematic measures of disparity selectivity using dynamic random dot stereograms (dRDSs), in which a uniform horizontal disparity was applied to all of the dots (uniform disparity stimulus). For all experiments using a dRDS, the dot size ranged from 0.09 to 0.2° (chosen according to which dot size produced the strongest response). The stimulus contained both black and white dots (density, 40%) with the same mean luminance as the gray background. When measuring disparity selectivity, the stimulus disparity ranged from −1.5 to 1.5° of visual angle and was applied to a circular patch of dots 5° in diameter. The disparity stimulus was surrounded by a 6.5° background of uncorrelated dots (eliminating any monocular cues to disparity). Initially, if the responses to the random dot stimuli used to assess disparity tuning were all weak, we rejected the cell and searched for a more responsive cell. After recording from several cells (18 of 139), it became clear that some cells responded strongly to a cyclopean edge stimulus even when they gave very weak responses to RDS stimuli containing a uniform disparity. Thus, by requiring a response to uniform disparity, we may have been biasing our sample against neurons that respond most strongly to cyclopean edges. Accordingly, after characterizing the tuning curve for uniform disparities, we probed each cell with stimuli containing a cyclopean edge, manually controlling the disparities and the orientation of the edge. If we found no random dot stimulus that could elicit at least 10 spikes/s, we did not record any quantitative data.

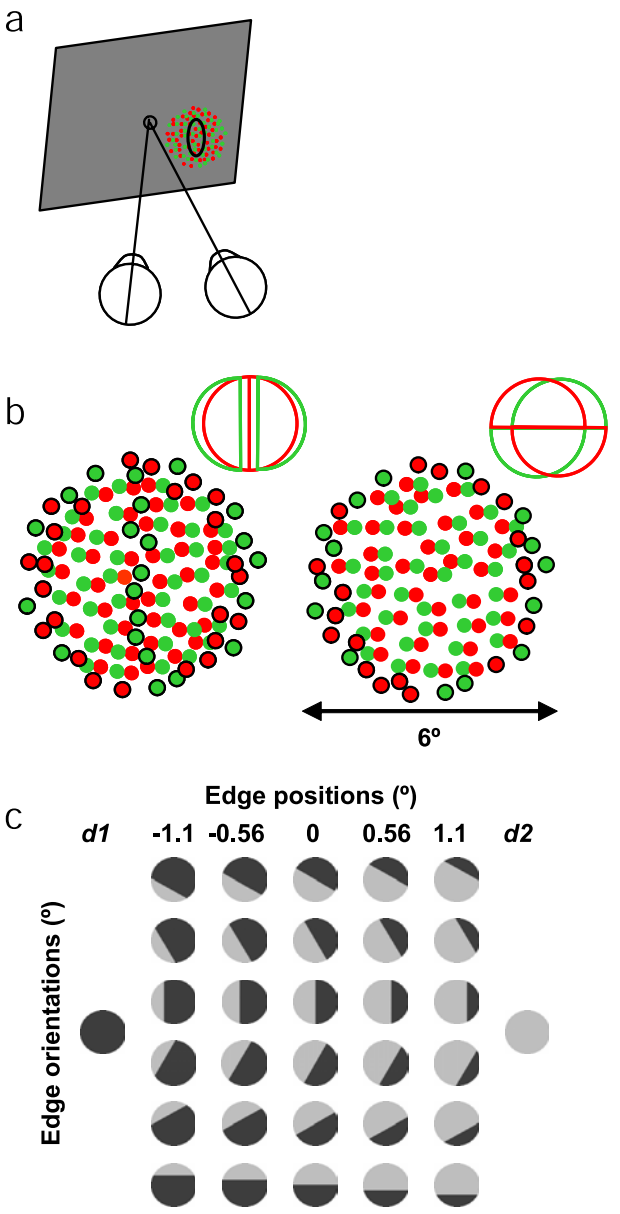

Figure 1. Experimental setup. ***a***, Monkeys fixated on a central fixation spot while the stimulus was centered on the receptive field (indicated by the solid black line). Receptive fields were located between 1 and 10° from the fovea in the right visual field. The stimulus was a black and white RDS containing a cyclopean edge created by applying two different disparities to the dots. The actual stimulus contained only black and white dots on a gray background; color is used in ***a*** and ***b*** for illustrative purposes only (red and green represent the views of the right and left eyes, respectively). ***b***, Reproduction of a stimulus containing a vertical edge (left) and a horizontal edge (right). The line drawings inset to the top right of the stimulus drawings illustrate schematically the displacements that were applied to different regions of the stimulus of each eye. The green dots have been shifted in opposite directions on either side of the cyclopean edge, to produce opposite horizontal disparities across the edge. For the vertical edge (left), this shift results in a gap in the green dots along the location of the cyclopean edge, as shown in the line drawing. The gap is filled with uncorrelated dots (identified here with a black boundary). Note that any step change in horizontal disparity across a vertical border inevitably results in uncorrelated dots (this is not peculiar to our stimulus generation method). When a horizontal disparity step occurs across a horizontal boundary, however, no "gap" is created by the displacement; thus, uncorrelated dots are not present. In all cases, we added uncorrelated dots around the margins of the stimulus so that no monocular displacement was ever present. ***c***, We measured the cyclopean edge response for six equally spaced orientations (rows) and five different edge positions for each orientation, 0.55° apart (columns). Dark and light gray shading represents different disparities (d1 and d2, respectively). Each orientation and edge position was measured for both signs of the cyclopean edge (data not shown); opposite sign edges were created by simply swapping the disparities across the edge.

Measuring cyclopean edge selectivity. We measured responses to cyclopean edges defined by two surfaces that differed from one another only in their horizontal disparity. The stimulus was a circular dRDS 6° in diameter, where the central 5° contained two contiguous regions defined by different disparities. The border between the surfaces formed an edge in depth (see Fig. 1*b* for an illustration of the stimulus). Because of the disparity step, this border region inevitably contained dots in one eye's image that had no partners in the other eye (uncorrelated dots). Because all disparities were applied horizontally, the size of the uncorrelated region varied with orientation and was largest for vertical edges and nonexistent for horizontal edges. Finally, to ensure that the monocular appearance of all stimuli was identical, the outer 1° was filled with uncorrelated dots.

If the cell exhibited disparity selectivity for uniform disparities, we selected a pair of disparities that were within 0.5° of the peak of the tuning curve to define the cyclopean edge. We tested several different disparity configurations, often in the same cell, including edges defined by the peak and null disparities and edges defined by disparities that produced roughly equal response rates. If a cell showed weak or flat disparity tuning, we selected disparity pairs that were nearly symmetrical about zero.

Figure 1*c* schematically illustrates the range of orientations and edge locations in our stimulus set. The cyclopean edge was presented at six orientations spaced 30° apart, ranging from 0 to 150°. Each oriented edge was presented at five different locations (−1.1, −0.55, 0, 0.55, and 1.1° of visual angle relative to the center of the stimulus) and in two different sign configurations (where "sign" describes which side of the edge was in front). We also measured the response to three uniform control stimuli: the two uniform disparities used to define the edge and a stimulus consisting entirely of uncorrelated dots. There were a total of 63 stimuli.

Each stimulus was presented a minimum of four times, although we collected eight or more stimulus presentations whenever possible (a mean of 5.9 repetitions per stimulus).

Data analysis. Our first goal was to identify cells that responded to the cyclopean edge in a way that cannot be explained by V1-like receptive fields. To do this, we simulated V1 cell responses to a cyclopean edge, based on the assumption that the disparity responses of V1 cells are well described by the binocular energy model (Adelson and Bergen, 1985; Ohzawa et al., 1990; Fleet et al., 1996; Ohzawa, 1998). If V1 cells behave as energy units, their responses to stimuli containing several disparities can be predicted from their responses to the component disparities. The prediction is calculated by summing the responses to components, weighted by the proportion of the receptive field each component covers. For a cyclopean edge defined by two disparities, this sum has three components: the response to the two disparities and the response to the uncorrelated dots. The receptive field envelope was modeled as a two-dimensional Gaussian with SDs σ_x,σ_y.

Changes in the orientation and position of an edge therefore affect the response of energy model-like cells because of changes in the proportions of the different disparity components stimulating the receptive field. We examined this in model cells with a range of receptive field sizes (σ_x,σ_y ranged from 0.2 to 1.5°), elongations (ratio of height to width ranged from 1 to 3), orientations, and positions relative to the center of the stimulus.

A full description of the results of these simulations is presented in the Results. In brief, these simulations demonstrate that the binocular energy model can produce the appearance of orientation tuning for a cyclopean edge. However, the model response to a cyclopean edge never exceeds the largest response to the individual components; for this reason, we always measured the response to these components (the uniform control stimuli) whenever we measured responses to cyclopean edges. Any V2 cell that responds more strongly to the cyclopean edge than to the individual components of the edge cannot be reconciled with the binocular energy model and represents some further specialization of disparity processing.

Because we examined so many different conditions (60 combinations of orientation and location), applying a simple test (e.g., a *t* test) to compare each cyclopean edge with the control stimuli was impractical (primarily because the correction for multiple comparisons greatly reduces statistical power). We therefore devised a simple metric that could be applied to all the responses at once. This metric measures the magnitude of cyclopean edge responses as the sum of all activity that exceeds the largest response to any component disparity (two uniform disparity stimuli and an uncorrelated RDS). This measure is always zero for energy units with no noise and in the presence of noise is small with no systematic variation as a function of orientation. Values of this metric that are significantly greater than zero cannot be explained by the binocular energy model. Such enhancement therefore represents a response that is specific to the "cyclopean" structure of the stimulus, and so we call it cyclopean enhancement.

We calculated the total value of the cyclopean response enhancement summed across all stimuli as follows:

$$r_{\mathrm{EDGE}} = \sum_{\theta} \sum_{\delta} \max(R_{\theta,\delta}, [R_{\mathrm{d1}}, R_{\mathrm{d2}}, R_{\mathrm{uc}}]) - \max([R_{\mathrm{d1}}, R_{\mathrm{d2}}, R_{\mathrm{uc}}]),$$

where $R_{\theta,\delta}$ is the response to a cyclopean edge with a given orientation θ and position δ and $[R_{\mathrm{d1}}, R_{\mathrm{d2}}, R_{\mathrm{uc}}]$ are the responses to each of the three uniform disparity control stimuli (two component disparities and uncorrelated dots). Here, any edge stimulus producing a response that exceeds the response to all control stimuli contributes a positive value to r_{EDGE}, whereas responses below the maximum control response contribute zeros to the r_{EDGE} calculation. Thus, r_{EDGE} represents the magnitude of cyclopean enhancement summed across all edge orientations and positions. Because a single value of r_{EDGE} is calculated across all conditions, it is not subject to the multiple comparison problem encountered by testing each orientation and/or position response individually. Ideal noise-free cells that did not respond to the cyclopean edge would have an r_{EDGE} value of 0, whereas larger values indicate responses to one or more cyclopean edge stimuli that were greater than could be explained by any of the control stimuli.

For cells in which r_{EDGE} was >0, we used a resampling technique to determine whether r_{EDGE} was greater than would be expected by chance. Because the calculation of r_{EDGE} involves a response rectification (r_{EDGE} includes only the activity greater than the control response), response noise results in (small) positive values of r_{EDGE}. For this reason, we could not simply resample the data and ask whether r_{EDGE} was reliably greater than zero; instead, we asked how large r_{EDGE} could be under the null hypothesis (H_0) if the true response contained no cyclopean edge enhancement [$r_{\mathrm{EDGE}}(H_0)$].

Simulations with artificial data showed that the specific formulation of this null hypothesis was critical. A conservative approach would be to assume that every response was drawn from a population with a mean of $\max[R_{\mathrm{d1}}, R_{\mathrm{d2}}, R_{\mathrm{uc}}]$ (the maximum control response). However, this overestimates the value of $r_{\mathrm{EDGE}}(H_0)$ in energy model neurons that respond differently to the two disparities defining the edge. This is because many edge configurations systematically produce responses lower than the maximum control response (see simulations presented in Results), and adding noise to artificially high values tends to inflate the estimated value of $r_{\mathrm{EDGE}}(H_0)$. Our simulations with artificial data showed that this effect could profoundly affect the statistical power of the metric.

We therefore formulated the null hypothesis that the data had been generated by a V1-like energy model cell. Under this hypothesis, the response for each stimulus orientation can be described as the sum of two functions. The first function is a cumulative Gaussian that describes the response to the two component disparities as a function of position. The values at the extremes of this function are given by the responses to the uniform disparity controls. The second function describes the response to uncorrelated dots as a Gaussian function of position. The amplitude of this Gaussian is determined by the response to uniform uncorrelated dots and the width of the uncorrelated region relative to the receptive field. Note that this width varies with stimulus orientation. The cumulative Gaussian and the Gaussian share the same center and SDs (reflecting the receptive field size and location), and values for these two parameters were determined with a least-squares fit. The fit also included a free term for a final output exponent, maximizing the quality of the null hypothesis fit to the data.

Each orientation was fit separately, allowing both the SD and the center of the cumulative Gaussian to vary, but both disparity signs were fit

with a single parameter set. By adding noise samples to the fitted functions, we were able to use these fits to estimate the value of r_{EDGE} that could have been generated by chance. Noise samples were generated by drawing random samples with replacement from the residuals in our original data set. The set of residuals was calculated by pooling the residuals for each of the 63 data points around its own mean. We first eliminated the dependence of the variance on the mean firing rate by performing all resampling calculations on the square root of the firing rate (Prince et al., 2002). Finally, we calculated r_{EDGE} (H_0) for the resampled data and repeated this process 1000 times to generate a distribution of values expected under the null hypothesis. If the measured value of r_{EDGE} was >95% of the resampled values of r_{EDGE} (H_0), we considered the cyclopean enhancement to be significant.

This method of resampling, in which we generate a distribution of values from a null hypothesis, is unusual. We explored many metrics based simply on resampling the data in the usual way, but simulations on artificial data revealed problems with all of them. Two factors make the problem difficult. First, we need a metric that looks only at responses exceeding the uniform disparity controls. Because this involves rectification, the expected value of such metrics is always greater than zero. Second, the size of the responses that can be generated by noise in the energy model depends on the difference in the responses to the component disparities (as explained above), so there is no fixed value that can be used as a criterion. In extensive simulations with artificial data, the method we present here was the only one that gave consistently appropriate false positive rates, between 3 and 5%.

For some cells, we measured the responses to cyclopean edges in more than one experiment, each experiment using different disparity pairs to define the edge. To determine the overall significance of the cyclopean edge response for all disparity pairs, we calculated the product of the probabilities ($p_j = p_1 \times p_2 \times \ldots p_k$, where k is the number of experiments run on a particular cell) and determined whether the resulting value could have been observed by chance. The probability that a given product of probabilities could have been observed by chance (P_j) is as follows:

$$P_j = p_j \sum_{i=1}^{k} \frac{\ln(p_j)^{i-1}}{(i-1)}.$$

If P_j was <0.05 but no single experiment passed the individual test (indicating very weak tuning), the data were not included in subsequent analyses of selectivity for cyclopean edge orientation.

Analysis of orientation selectivity. For cells that showed significant cyclopean enhancement, we asked whether the response was selective for the orientation of the cyclopean edge. In this analysis, we wanted to isolate the orientation modulation that was specific for the cyclopean edge. Therefore, we first compared the best V1 energy cell fit for a given orientation (H_0, as used above to test the significance of r_{EDGE}) to the observed response for that edge orientation. The deviations of the observed response from H_0 represent that portion of the response that cannot be explained by a Gaussian receptive field with uniform disparity tuning. The mean of these deviations across edge position therefore provides an estimate of the entire response to the cyclopean edge, so we call this mean the cyclopean edge response. This is similar to "cyclopean enhancement" defined earlier, but it includes all deviations from the fit, rather than only those deviations that produce responses greater than the uniform control stimuli.

To quantify orientation tuning, we calculated the cyclopean edge response as a function of orientation (r_θ), treating opposite edge signs as orientations that were 180° apart:

$$r_\theta = \frac{\sum_{\delta} (R_{\theta,\delta} - H_{0\theta,\delta})}{N},$$

where N is the number of edge positions that we measured. r_θ could be either positive, reflecting enhanced responses to cyclopean edges, or negative, reflecting cyclopean edge suppression.

We then calculated the vector average of r_θ, $|\bar{r}_x, \bar{r}_y|$, where

$$\bar{r}_x = \frac{\sum_{\theta} r_\theta \cos\theta}{\sum_{\theta} |r_\theta|}; \bar{r}_y = \frac{\sum_{\theta} r_\theta \sin\theta}{\sum_{\theta} |r_\theta|}.$$

The direction of the vector average provides an estimate of the preferred orientation of the cyclopean edge stimulus ($\theta_{pref} = \arctan \bar{r}_y/\bar{r}_x$), and the circular variance of the vector average estimates the strength of orientation selectivity ($cv = 1 - \sqrt{\bar{r}_x^2 + \bar{r}_y^2}$). If the response is driven entirely by the responses to the component disparities, r_θ will be 0 for each orientation, cv will be 1, and θ_{pref} will be undefined. A $cv < 1$ indicates that the cell does modulate its response to a cyclopean edge as a function of orientation. cv can be as small as zero if only a single orientation produces cyclopean enhancement.

To determine whether the orientation selectivity of the cyclopean edge response was statistically significant, we resampled the data after pooling the residuals for each of the 63 data points around its own mean. Using the resampled values, we calculated 1000 values of θ_{pref}. If 95% of the resampled values of θ_{pref} fell within a range of 180°, this means that there is a vector onto which 95% of the resampled values have a positive projection, so we take this to indicate significant orientation tuning at the 5% level. We refer to the angle containing 95% of the directions of the resampled vector averages as the 95% confidence angle (α_{95}).

If cells respond strongly to both signs of the disparity edge (i.e., the orientation tuning has two peaks 180° apart), the opposite sign responses tend to cancel in the calculation of the vector average of r_θ. We dealt with this problem in the usual way, treating orientations 180° apart as the same angle (done by calculating the vector average after doubling all angles, then halving the resulting value of θ_{pref}).

We used this alternate measure of orientation selectivity only for cells that gave a statistically reliable response to edges of the non-preferred sign. Measuring the statistical reliability of non-preferred sign responses required some interpolation. The preferred orientation θ_{pref} often takes values that do not correspond exactly to any one stimulus. Thus, to determine the response at the same orientation, but non-preferred sign, we first calculated r_{EDGE} as a function of orientation:

$$r_{EDGE}(\theta) = \Sigma_\delta \max(R_\theta, \delta, [R_{d1}, R_{d2}, R_{uc}]) - \max([R_{d1}, R_{d2}, R_{uc}]).$$

To obtain the response at the non-preferred sign of the preferred orientation, we smoothed $r_{EDGE}(\theta)$ with a coarse wrapped Gaussian ($\sigma = 22°$) and extracted the value at $\theta_{pref} + 180°$. A measured value of $r_{EDGE}(\theta_{pref+180})$ greater than expected under the null hypothesis for >95% of the resampled data sets (using the same null hypothesis as was used to test the significance of r_{EDGE} above) indicates a significant response to the non-preferred sign.

Although the confidence angle α_{95} and the circular variance provide an estimate of how strongly tuned a neuron is for orientation, they do not provide detailed information about the pattern of orientation tuning. Specifically, for cells that respond significantly to both signs of an optimally oriented edge, we would like to be able to distinguish between cells that are truly orientation selective for both signs of an edge and cells that respond equally well to orthogonally oriented edges as they do to the non-preferred sign of an edge at the preferred orientation. Thus, we compared the cyclopean edge response for the non-preferred edge sign ($r_{\theta pref+180}$) and for edges oriented orthogonally to the preferred orientation (averaged over sign, $r_{\theta orth} = (r_{\theta pref+90} + r_{\theta pref-90})/2$). Significance was measured by calculating $r_{\theta pref+180}$ and $r_{\theta orth}$ on each resample after subtracting H_0 for that resample.

Analysis of position and sign invariance. For cells that were reliably orientation selective for both signs of the edge, we then determined whether the response to both signs occurred for an edge at the same spatial location (i.e., was position invariant). This analysis was performed on the data for the stimulus orientation that was closest to θ_{pref} and $\theta_{pref} + 180°$. Slightly different analyses were applied for both raw response rates (mean spike rate) and cyclopean edge responses (i.e., after subtracting the estimated response to the uniform disparities, H_0). To

determine whether there were changes in the peak of the raw response, we measured the distance between the edge position that produced the maximum response for the preferred sign and the position that produced the maximum response for the opposite sign. We refer to this distance to as $\Delta\delta^{max}$. Significance was determined by resampling ($p < 0.05$ if 97.5% of resampled values have the same sign for $\Delta\delta^{max}$).

To quantify the preferred edge location for that part of the response that was specific to the cyclopean edge, we first subtracted the estimated binocular energy cell response (fitted H_0, removing the response to the uniform disparity stimuli). We then calculated the center of mass (across position) of the cyclopean edge response for each sign of an edge at the preferred orientation:

$$COM_\theta = \frac{\sum_\delta \delta \, |R_{\theta,\delta} - H_{o\theta,\delta}|_+}{\sum_\delta |R_{\theta,\delta} - H_{o\theta,\delta}|_+},$$

where $|x|_+$ means half-wave rectification of x. θ could be either θ_{pref} or $\theta_{pref+180}$. The center of mass measurement provides a more robust measurement of the preferred edge location because it makes use of all data points that exhibit edge enhancement for a given orientation. It also allows for values that are not limited by the spacing of the measurements. We then measured the difference between the center of mass for the opposite edge sign responses ($\Delta COM = COM_{\theta pref} - COM_{\theta pref+180}$). Significance was determined by repeating this calculation on 1000 resampled data sets.

Finally, we tested whether the distribution of ΔCOM across the whole population of cells was larger than expected at random by using the resampling distributions to estimate the population distribution expected by chance. To do this, we first subtracted the mean of each cell's resample distribution, corrected for the loss of one degree of freedom by multiplying by

$$\sqrt{\frac{2n-1}{n-1}}$$

(where n is the number of data points contributing to the mean) and then summed these distributions from all cells. We compared this re-centered distribution against the original distribution of all resampled values (collapsed across cells). The Wilcoxon sign-rank test provides a nonparametric estimate of the probability that these two distributions come from the same underlying distribution.

Measuring orientation tuning for contrast-defined contours. For a subset of cells, we measured orientation tuning to contrast-defined stimuli, to compare this with selectivity for cyclopean contours. Orientation tuning for luminance contrast was measured using gratings of the optimal spatial frequency (determined manually) or bars with the optimal width, depending on which stimulus produced a stronger response modulation as a function of orientation. To avoid artifacts in the orientation tuning curve attributable to binocular interactions, we measured tuning in the dominant eye, determined by which eye produced a larger orientation modulation.

Although we measured orientation tuning for cyclopean edges at discrete edge positions, we measured orientation tuning for luminance contrast using bars or gratings that drifted across the receptive field at the preferred speed of the neuron (determined manually). This difference was necessary because cortical cells respond poorly to static contrast stimuli (Hawken et al., 1996), producing only a transient response. In the cyclopean stimuli, although the edge was static, the dynamic random dots contained temporal energy that produces a sustained response. Because orientation tuning has been shown to be independent of temporal frequency over a wide range (Moore et al., 2005), we do not expect this difference in stimulus parameters to substantially affect the results.

Each contrast stimulus was presented at nine orientations 22.5° apart, spanning 180° of orientation (because we were only interested in the axis of orientation). We calculated the vector average and *cv* on doubled angles. If a neuron was direction selective (determined manually), the stimulus orientations were centered on the preferred direction.

Results

Simulation results

The goal of this work was to assess the pattern of responses to edges defined solely by differences in horizontal disparity (cyclopean edges) in individual V2 neurons of the awake, behaving macaque. To identify neurons that selectively responded to such stimuli, we first needed to understand the pattern of responses that would be expected from a V1-like binocular energy cell that responds only to the component stimuli. Binocular energy cell responses to cyclopean edges are described by a linear combination of the responses to the three component stimuli (two component disparities used to define the edge and uncorrelated dots that occur at the edge location).

To illustrate how V1-like neurons might appear selective for the orientation of a cyclopean edge, we calculated the responses of binocular energy model cells to cyclopean edges with various orientations, positions, and disparity combinations. Figure 2*a* illustrates the disparity tuning of one such model cell, with the disparities used to define the cyclopean edge test stimuli used in Figure 2*b–d* marked with dots. The results of three simulations using cyclopean edges are shown in Figure 2*b–d*. In Figure 2*b*, the stimulus is centered on the receptive field. The model cell modulates its response with cyclopean edge orientation. This weak modulation is caused by the uncorrelated region that occurs at the border between the two disparities. Because we applied only horizontal disparities, the size of this region changes as a function of orientation. The uncorrelated region is largest for vertical edges and disappears for a horizontal edge. As the width of the uncorrelated region grows, the model response becomes closer to that produced by an uncorrelated stimulus. The size of this modulation depends on the strength of the response to uncorrelated dots, relative to the strength of the response to the uniform disparities defining the edge stimulus. If the uncorrelated rate is significantly higher or lower than the response to the uniform disparity components, the modulation can appear quite strong, as shown in Figure 2*c*. However, the response to the cyclopean edge never exceeds the maximum response to the set of component disparities (two uniform disparities and the uncorrelated stimulus).

In Figure 2*d*, the stimulus is not perfectly centered on the receptive field of the model cell. For this reason, the proportions of each of the component disparities falling within the receptive field change considerably as a function of orientation. As a result, the cyclopean edge response of the model cell seems to be strongly orientation tuned. However, if the response is measured at several locations for each orientation tested (shown as a pseudocolor plot in Fig. 3), it is possible to see that the changes in response with orientation are an artifact of the mis-centering. In this plot, the response magnitude is given by pixel color, the angle between a given pixel and the horizontal indicates the orientation of the edge stimulus, and the edge position is mapped onto radial distance. Stimuli 180° apart on this plot have the same edge orientation, but the component disparities are on opposite sides of the edge (which we refer to as opposite disparity signs of the edge). The central disc and outer annulus indicate the response to the component disparities. The response to uncorrelated dots is shown in the corners of the image.

The orientation tuning curve shown in Figure 2*d* corresponds to a ring in the response surface shown in Figure 3 (indicated by a dotted gray line). However, if we take radial slices through the data, as shown to the right of and below the pseudocolor plot in Figure 3, it becomes clear that as the cyclopean edge sweeps from

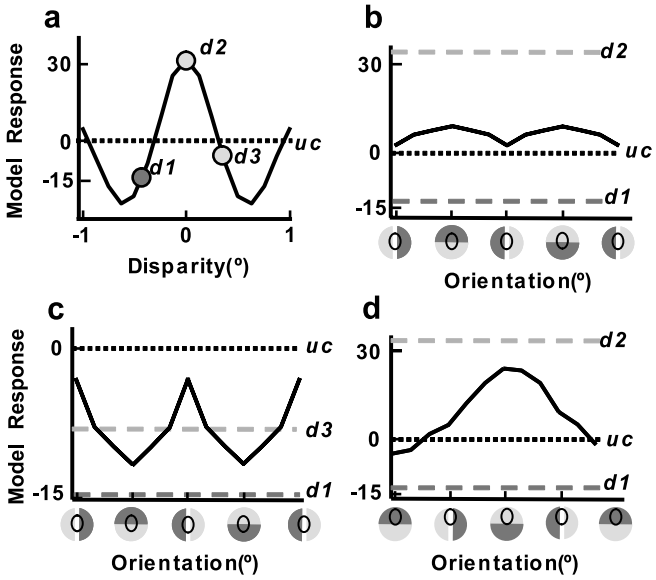

Figure 2. Responses of the binocular energy model to stimuli containing cyclopean edges. ***a***, Disparity tuning of the model cell. The disparities used to define the cyclopean edge in ***b*** and ***d*** are marked with dots at −0.4° (d1; dark gray) and 0° (d2; light gray). The disparities used to define the edge in ***c*** are shown with dots at −0.4° (d1; dark gray) and +0.4° (d3; light gray). The dotted black line indicates the response of the model cell to uncorrelated stimuli. ***b–d***, Tuning of the binocular energy model cell for the orientation of a cyclopean edge (solid black line). As in ***a***, the dotted black line indicates the response of the model cell to uncorrelated dots (uc). The dashed gray lines indicate the responses to the component disparities d1 = −0.4 (dark gray) and d2 = 0 (***b***, ***d***) or d3 = +0.4 (***c***) (light gray). The line drawings along the *x*-axis represent the stimulus and receptive field at instructive edge orientations. Light and dark gray shading represent the disparities used to define the edge. The receptive field is shown with a black ellipse. The model V1 cell responds according to the proportions of the different disparities appearing in the receptive field. ***b***, ***c***, Applying different horizontal dot displacements to the right and left of the stimulus creates a vertical cyclopean edge, with a gap at the location of the edge in the view of one eye, which is filled with uncorrelated dots. Applying the same two disparities to the top and bottom of the stimulus creates a horizontal cyclopean edge with no gap at the edge location. In ***b***, the model cell responds relatively weakly to an uncorrelated stimulus. Because the response of the model cell is determined by the combination of stimuli in its receptive field, it responds more strongly to a horizontal edge than to a vertical edge. In contrast, in ***c***, the strongest response of the model is to uncorrelated dots, and the cyclopean edge response shows sharp increases for non-horizontal edges. The size of the uncorrelated region changes smoothly as a function of orientation, causing the response of the model cell to change as a function of orientation. ***d***, Mis-centering the receptive field on the stimulus causes the relative proportions of the two disparities covering the receptive field to change with the orientation of the cyclopean edge. In this example, the receptive field sits over the top half of the stimulus (as shown schematically in the line drawings on the *x*-axis). The horizontal edge stimulus produces a strong response when the 0° disparity (light gray) is in the top half of the stimulus and a much weaker response when the disparities are swapped.

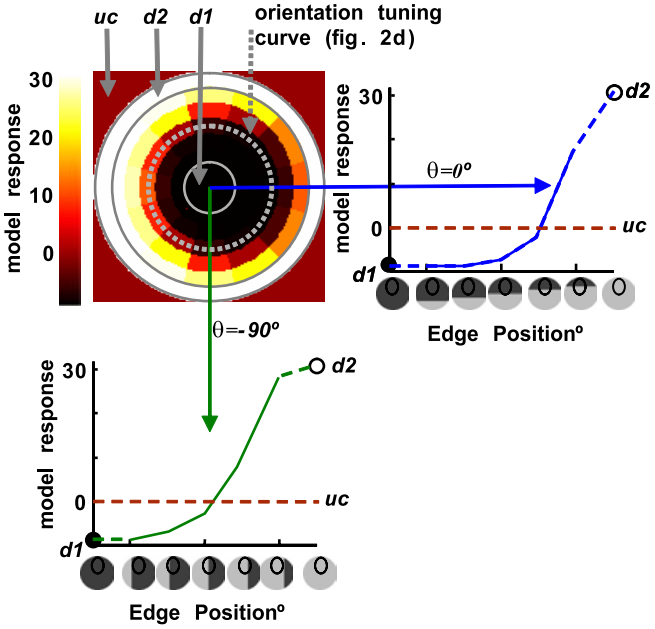

Figure 3. Model responses to all cyclopean edge orientations and positions for the stimulus/receptive field configuration shown in Figure 2*d*. In the pseudocolor plot, the angular position of a patch (relative to the horizontal) represents stimulus orientation, whereas radial distance from the center represents edge position. The dotted gray line marks the middle of the five concentric rings, representing a cyclopean edge in the center of the stimulus and corresponding to the orientation tuning curve shown in Figure 2*d*. The central disc and the outermost rings (delineated by solid gray lines) represent the response to control stimuli with uniform disparity. These conditions can be viewed as edge locations that lie outside the stimulus, as reflected by their radial location. The corner regions outside the outermost ring represent the response to uncorrelated dots (uc). The mapping between radial location and edge position can be more clearly seen in the cross sections shown below and to the right of the pseudocolor plot. The cross section shown to the right represents the response of the model for a cyclopean edge oriented at 0°. The stimulus icons along the *x*-axis indicate the edge orientation and position for each point in the plot. The two uniform horizontal disparities used to define the edge, d1 and d2, are shown as the extrema of the position tuning curve, and the symbol color matches the color for these data in the pseudocolor plot. Note that d1 and d2 are connected to the position tuning curve using dashed lines, because these controls correspond to a range of edge locations falling outside the stimulus. The dashed line represents the response to uncorrelated dots. A cross section for an orthogonally oriented edge ($\theta = -90°$) is shown below the pseudocolor plot, using the same plotting conventions. In both cross sections, it is clear that the cyclopean edge response never exceeds the response to the most effective uniform component disparity (d2 in this example).

one side of the stimulus to the other, the response always modulates between the responses to the two component disparities. The model cell never responds better or worse to a cyclopean edge than it does to the uniform disparities used to define the edge. Thus, although the model cell modulates its response to oriented cyclopean edges at any one edge position, the modulation can be explained as a linear sum of its responses to the component disparities alone.

V2 results

Magnitude of cyclopean edge response

These simulations indicated that responses that exceed those to the uniform disparity controls (including uncorrelated dots) must be specific to the cyclopean edge. Thus, we focused on identifying neurons, which had responses to cyclopean edges were significantly enhanced relative to the responses to the component control stimuli. Overall, we studied 139 V2 neurons that met our inclusion criteria (producing a minimum of 10 spikes/s to at least one random dot stimulus and allowing a minimum of four repetitions of each stimulus). Figure 4 shows the response of one example neuron as a function of edge position for an edge at the preferred orientation of the neuron (solid blue line, ±1 SEM). The dashed lines show the response to the two disparities used to define the edge (blue lines) and a stimulus containing uncorrelated dots (black line). To determine whether cyclopean enhancement was significant for a given cell, we first calculated the sum of all responses that exceeded the response to the uniform controls (r_{EDGE}), collapsing across both edge position and orientation. In Figure 4, the red lines show the contribution to r_{EDGE} made by responses to a single stimulus orientation; each line indicates the magnitude of the response that is larger than d2 (the largest control response). To test the overall significance of cyclopean enhancement for a given cell, all such responses (above the uniform disparity controls) were summed across all orientations and edge positions. We used resampling to determine whether

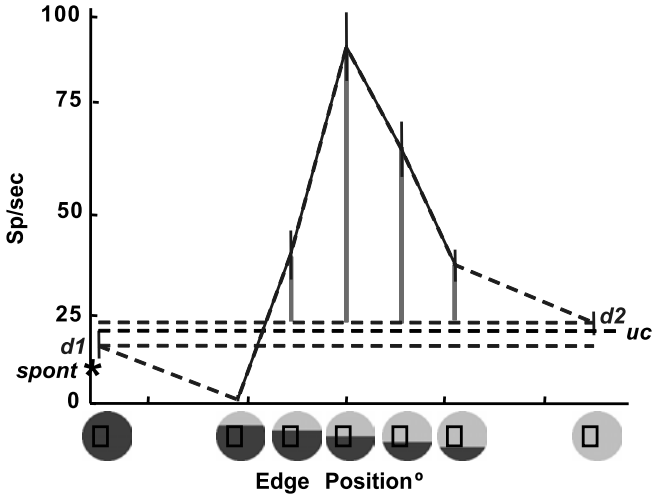

Figure 4. Example of cyclopean enhancement at a single edge orientation. The solid blue line plots the firing rate as a function of edge position for the preferred orientation (±1 SEM) of the cell. Dashed blue lines indicate the response to the uniform disparity controls (d1 and d2), whereas the dashed black line represents the response to a stimulus containing uncorrelated dots (uc). The receptive field is shown as a black rectangle superimposed on the stimulus icons along the *x*-axis. For this and all other example cells, the receptive field was measured using narrow strips of grating such as those described by Read and Cumming (2003). The rectangle represents the region enclosing all responses >10% of maximum. The spontaneous firing rate is indicated by the black asterisk on the *y*-axis. Vertical red lines indicate the extent of cyclopean enhancement (responses in excess of any uniform control). The summed length of the red lines is the total contribution from this orientation to our measure of cyclopean enhancement, r_{EDGE} (see Materials and Methods). The full value of r_{EDGE} was summed across all orientations. Sp/sec, Spikes per second; spont, spontaneous.

r_{EDGE} was greater than expected from a V1-like receptive field with uniform disparity selectivity (see Materials and Methods). Figure 5*a* shows the distribution of r_{EDGE} across our population of V2 cells. Red bars represent the 65 of 139 cells that showed significant cyclopean enhancement ($p < 0.05$). There is clearly a continuum from relatively weak but consistent edge responses (minimum significant $r_{EDGE} = 2.6$), to robust responses that dwarf the uniform disparity controls [such as the examples in Figs. 6 ($r_{EDGE} = 73.49$) and 7 ($r_{EDGE} = 333.8$)]. Such a continuum of tuning is consistent with the idea that cyclopean edge tuning is a property that emerges in V2. A similar metric was also used to identify responses significantly lower than could be explained by a V1-like disparity-selective cell. Such cyclopean suppression was uncommon (7 of 139), and weaker than cyclopean enhancement, and so will not be explored further.

We calculated r_{EDGE} to determine the statistical significance of cyclopean enhancement. However, its value does not clearly indicate the magnitude of cyclopean enhancement relative to the responses to stimuli of uniform disparity. To explore this relationship, Figure 5*b* compares the maximum cyclopean edge response to the best response to any of the control stimuli. Significant cyclopean edge responses naturally tend to lie well below the identity line. (However, in two cases, very small values of r_{EDGE} are significant, because responses similar in magnitude to a control response occurred at locations that cannot be explained by a receptive field with uniform disparity selectivity.) On average, these cells responded more than twice as well to a cyclopean edge than they did to the best uniform disparity control stimulus. This strong response enhancement clearly reflects a specialization for something other than a uniform disparity stimulus.

The effects of such a specialization should also be evident when considering responses to a wider set of uniform disparities. The simplest form of feedforward processing that might produce cyclopean responses such as those we document here would sum inputs from V1 neurons that had different preferred disparities and different receptive field locations. For such a neuron, any stimulus of uniform disparity would necessarily be suboptimal, because it cannot optimally activate each subunit. As a result, we would expect the optimum cyclopean edge to produce stronger activation than any uniform disparity. Figure 5*c* compares the maximum response to a cyclopean edge with the maximum response to any uniform disparity (from the disparity tuning curve) for the subset of cells for which we had both disparity and cyclopean edge tuning using the same size stimuli ($n = 112$). Points plotted in red are those cells that showed significant cyclopean enhancement. Again, the red points tend to fall well below the identity line, indicating that they responded considerably better to the cyclopean edge than they did to any uniform disparity stimulus ($p < 0.001$, paired *t* test). In contrast, the blue points tend to cluster at or above the identity line, representing approximately equal response rates for uniform disparities and cyclopean edges ($p > 0.5$, paired *t* test). These results are consistent with the idea that any uniform disparity is a suboptimal stimulus for neurons that respond significantly to cyclopean edges.

Examples of cyclopean edge responses

The results above establish that even in our impoverished stimulus, in which no clear figure is defined, many V2 neurons show a response that is specific to cyclopean edges. Before turning to the population data, we first present three examples that illustrate the range of responses that we observed (Figs. 6–8). These examples illustrate how detailed examination of the responses allows us to distinguish signals that are cue invariant from those that could be explained by a simple convergence model.

Figure 6*a* shows all of the data for one experiment as a polar pseudocolor plot, similar to that shown in Figure 3. The striking feature in this data set is a marked peak in the response when the cyclopean edge is located near the center of the stimulus, with an orientation of 180°. No other combination of orientation/position produces a comparable response rate.

The elevated response to the preferred cyclopean edge stimulus can be more easily seen by examining the response to a single orientation of the cyclopean edge as a function of edge position, shown in Figure 6*b*. The ends of this curve show responses to control stimuli of uniform disparity (each end was one of the two disparities used to define the edge, d1 and d2), equivalent to an edge location far outside the receptive field. The dotted green line in Figure 6*b* shows our best estimate of the uniform disparity modulation that would be expected from a simple V1-like energy cell which transitions smoothly from d1 to d2.

However, for the stimulus orientation shown in Figure 6*b*, the response of the cell is much greater for an appropriately positioned cyclopean edge than to either d1 or d2. The only way in which a binocular energy model cell could produce a qualitatively similar response would be if it had an extremely high response to uncorrelated dots, but the response in Figure 6*b* clearly exceeds the response to a uniform stimulus of uncorrelated dots (dashed red line).

The significant cyclopean enhancement establishes that the responses in Figure 6 cannot be explained by a receptive field with uniform disparity selectivity. This is a conservative criterion, based only on edge stimuli that produce larger responses than any of the controls. It is important to recognize that the cyclopean edge may affect firing rates even for stimuli which produce responses smaller than the best response to a uniform control stim-

ulus. To analyze the entire cyclopean response, we compare the observed responses to our best estimate of a V1-like response to this stimulus (see Materials and Methods). We summarize the cyclopean edge response at each individual orientation, r_θ, by taking the average of the deviations from this fit across all edge locations. We then examine how this varies with stimulus orientation. Any significant variation of r_θ with stimulus orientation must be attributable to the cyclopean edge.

Figure 6*c* shows a polar plot of how r_θ varies with orientation. The preferred orientation θ_{pref} is estimated by calculating the vector average of r_θ over all orientations (Fig. 6*c*, $\theta_{pref} = 162°$). We estimated the reliability of θ_{pref} from the 95% confidence interval of the distribution generated by resampling ($\alpha_{95} = 18°$; see Materials and Methods); values <180° indicate statistically reliable orientation selectivity. We quantify the strength of the orientation signal with the circular variance (*cv*) of the data in Figure 6*c*. The circular variance is a routine measure of dispersion in circular data derived from the magnitude of the vector average (Mardia and Jupp, 2000). A circular variance of 1 represents a perfectly isotropic response, and 0 represents a response in which only a single orientation produced cyclopean enhancement. For the cyclopean edge data in Figure 6*c*, *cv* was 0.26.

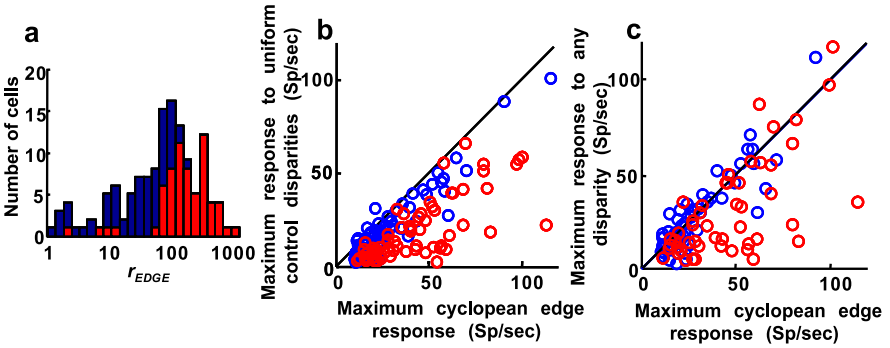

Figure 5. Strength of the cyclopean edge response. ***a***, Distribution of the magnitude of cyclopean edge response enhancement relative to the most effective uniform disparity control (summed over orientation and position). Red bars indicate responses that are significantly more responsive to a cyclopean edge stimulus than they are to any of the uniform stimuli used to define the edge ($p < 0.05$ by resampling). ***b***, Comparison of the maximum cyclopean edge response to the maximum responses for any of the three uniform control disparities (d1, d2, uc). Red data points indicate responses that were significant for cyclopean enhancement. Nonsignificant responses are clustered near the identity line, indicating that they responded about equally to the optimal cyclopean edge stimulus and the best control stimulus. Such equal responses in non-edge-specific cells are not surprising; they occur for locations in which the receptive field is mostly covered by one disparity. In contrast, significant responses (red data points) are generally found considerably below the identity line (paired *t* test, $p < 0.001$), reflecting much larger responses for their optimal cyclopean edge than for any of the control stimuli. ***c***, For a subset of cells ($n = 112$) for which we had both cyclopean edge and disparity tuning curves for the same size stimulus, we compared the maximum cyclopean edge response to the best response to any uniform horizontal disparity. As in ***b***, red data points indicate cells that give enhanced responses for cyclopean edges. In general, cyclopean edge-specific responses tend to be found below the identity line (paired *t* test, $p < 0.001$), indicating that they responded better to the cyclopean edge than to any uniform disparity stimulus (ranging from −1.5 to 1.5° of horizontal disparity). Sp/sec, Spikes per second.

The response shown in Figure 6*c* seems well suited to representing cyclopean contours, because it is well tuned for both orientation and edge position. To determine whether the representation of contour orientation generalized to other stimuli, we also measured the response of the cell to luminance gratings at the preferred spatial and temporal frequency (Fig. 6*d*). In this example, the orientation preference is very similar for these two very different stimuli, and the tuning is relatively sharp in both cases. Overall, this cell seems to be consistent with the idea of a sophisticated contour detector. However, these characteristics were elicited by an extremely impoverished stimulus, in which no figure was present, which suggests that they may be explained by the processing only of visual information within the receptive field. The similar responses to oriented contours defined by disparity and luminance contrast may be evidence for an organized convergence of input from V1.

Figure 7 shows data from a different neuron illustrating a second response pattern in which there is clear orientation tuning to cyclopean edges of both disparity signs (Fig. 7*a*,*c*, points plotted 180° apart). At first sight, this response appears a level of abstraction beyond that illustrated in Figure 6: it signals the orientation of the edge regardless of its disparity sign. However, closer inspection of the responses as a function of edge position (Fig. 7*b*) reveals that the cyclopean enhancement is maximal at very different edge positions, ~1.5° apart. The different preferred edge positions for opposite signs of an edge at the same orientation suggest that this cell is poorly suited to the function of a high-level contour detector. Conversely, this sort of relationship between position, orientation, and edge sign is readily explained by the simple feedforward convergence of two V1 disparity-selective cells (shown schematically in Fig. 7*d*), making a receptive field much like V1 simple cells, but in the disparity domain. As such, it would likely respond best to a bar at one disparity, on a background at a different depth. Unfortunately, because of experimental constraints, we were not able to test this hypothesis directly in this experiment.

Because this cell responded to both signs of a cyclopean edge, it required a slightly different measure of orientation selectivity. If a simple vector mean is calculated, the responses to opposite signs tend to cancel. This problem is readily solved by calculating the vector average after doubling the angles, then halving the angle of θ_{pref} (Mardia and Jupp, 2000). This measure of circular variance was 0.55 for the data in Figure 7. Similarly, the 95% confidence interval for the mean direction was small ($\alpha_{95} = 23°$), indicating that the orientation selectivity was reliable. In the population data that follow, neurons that had a statistically reliable response to both disparity signs (preferred and non-preferred) at the preferred orientation had all of their statistics performed on doubled angles, as in this example.

A final example (Fig. 8*a*) systematically produced higher responses than the uniform controls, but this enhancement occurred at all orientations, for both signs of the edge, and over a broad range of positions. The polar plot on the right in Figure 8*a* shows no clear orientation tuning, the circular variance is large, and the confidence interval for the preferred orientation is wider than 180°. Because this response is not orientation selective, it is impossible to say whether the enhanced response is specific to cyclopean edges, whether some other more optimal spatial configuration might exist (such as a center-surround type organization), or whether the response enhancement is simply a response to placing a mixture of disparities within the receptive field. Nonetheless, such an enhancement would not be shown by simple disparity detectors, so even this isotropic response represents something that would not be expected from V1 neurons.

However, the cyclopean enhancement shown in Figure 8*a* is

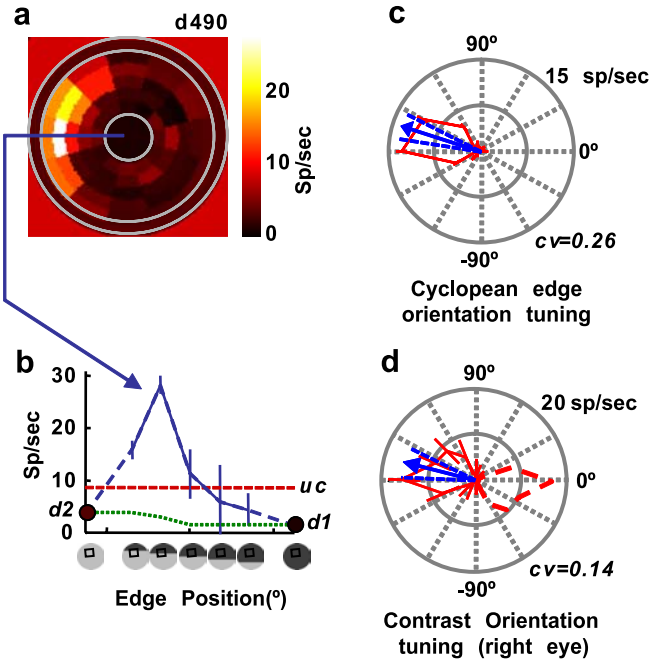

Figure 6. Example neuron showing orientation-selective cyclopean enhancement. ***a***, Response pattern for cyclopean edges with a range of orientations and positions. Plotting conventions are the same as for the pseudocolor plot in Figure 3. The solid blue line indicates the preferred orientation and sign of the cyclopean edge. ***b***, Cyclopean edge response as a function of edge position for the preferred orientation. Error bars indicate ±1 SEM. The component disparity responses (d1 and d2) are indicated at either end of the position tuning curve, and the uncorrelated control response (uc) is shown by the dashed red line. The dotted green line represents the best fit for a binocular energy model cell. The peak of the position tuning curve clearly exceeds the expected response from a binocular energy cell, as well as the response to any of the control stimuli. ***c***, Polar plot of cyclopean enhancement (red line). Although the units are spikes per second, these values are not raw response rates; rather, they indicate the difference between the response rate and the best estimate of the binocular energy cell response, averaged over position. Error bars indicate ±1 SEM. This neuron is only activated by one disparity sign, with a peak near the horizontal. The solid blue arrow marks the direction of the vector average, whereas the flanking dashed lines indicate the angle that contains 95% of these vectors across 1000 resampled values. The circular variance (cv) for this cell was 0.26. ***d***, Polar plot of the contrast response (mean spike rate, red line) as a function of orientation. Manual exploration indicated that this cell was not direction selective, so responses were only measured for stimuli between 90 and 270°. To avoid giving the visual impression of direction selectivity, the data are replicated with a dashed line in the right half of the plot. Plotting conventions are the same as in ***c***. Sp/sec, Spikes per second.

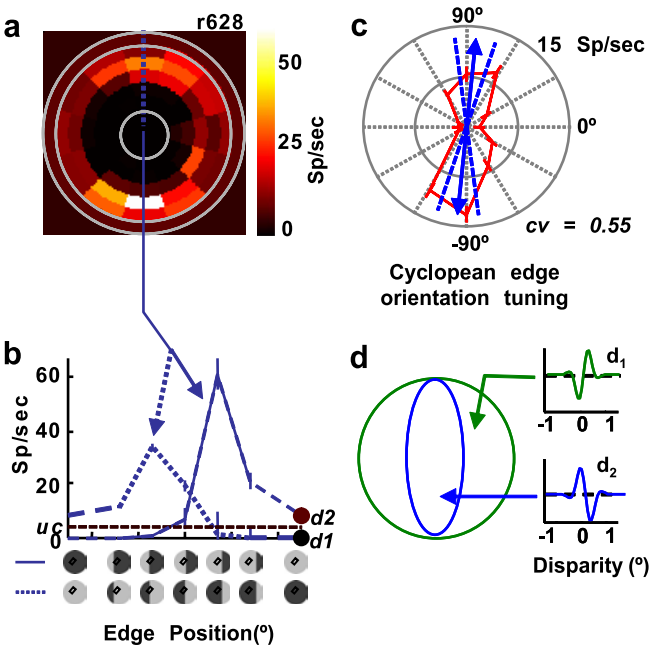

Figure 7. Example of an orientation-tuned response to both signs of a cyclopean edge. ***a–c***, Plotting conventions are similar to Figure 6. In ***a*** and ***b***, the solid and dotted blue lines indicate the responses to both signs of an edge at the preferred orientation. This cell clearly responds to both signs of an optimally oriented edge better than it does to any of the uniform control stimuli (d1, d2, and uc), although in different edge positions. The response to both signs of the edge can be seen in the polar plot shown in ***c***, in which there are peaks near both 90 and −90°. The vector average is shown extending in opposite directions, representing the use of the angle-doubled circular variance. ***d***, Schematic of the type of receptive field organization that could give rise to the pattern of responses seen in ***a***, with two subfields differing only in size and disparity preference. The different disparity tuning curves of the two subfields would produce a receptive field with an optimal response for the rectangular region with a disparity of −0.2°, surrounded by a background with a disparity of 0.2°. When tested with a single cyclopean edge, this receptive field would respond to both signs of the edge, in different locations. Sp/sec, Spikes per second.

highly sensitive to the disparities used to define the edge. Figure 8*b* shows that the same cell did not show any cyclopean enhancement when the disparities that defined the edge were changed by only 0.2°. Whereas the experiment in the top row shows cyclopean edge responses to all orientations and both signs, the experiment shown in the second row did not produce any significant cyclopean edge responses, despite the fact that the disparities used in the two experiments were similar (the disparities used for both examples are shown with different color markers in Fig. 8*c*). This striking specificity for the disparities used to define the edge makes it clear that this cell does not represent cyclopean contours in a cue-invariant way. Small changes in the stimulus defining a contour seem to be sufficient to abolish the response. This phenomenon is readily explained if the response comes from combining multiple subunits, each of which is sensitive to small disparity changes.

Population analysis

The above examples illustrate the range of responses to cyclopean edges seen in macaque V2. We highlighted several features of these data that can be used to evaluate whether the responses could be produced by a simple feedforward mechanism, and the extent to which they could support a cue-invariant contour representation. We now quantify each of these features across the population.

Orientation tuning

Previous studies have shown that V2 cells signal the orientation of cyclopean figures (von der Heydt et al., 2000). Here, we quantify these results for isolated cyclopean edges that are not part of a figure/ground stimulus. Figure 9*a* shows population data for the strength of orientation tuning (circular variance, *cv*), and its reliability (confidence interval for the mean vector direction, α_{95}). Neurons that responded to both signs of cyclopean edge are shown with squares, and their circular variance was estimated after doubling the edge orientations. The examples shown in Figures 6–8 are indicated with filled symbols. There is a continuum of responses between those that are strongly orientation tuned (Figs. 6 and 7, cyan and green filled symbols) and those that are not significantly orientation tuned (Fig. 8, red filled symbol). For the majority of neurons that showed cyclopean enhancement, the enhancement was reliably orientation selective (56 of 65), as indicated by their location below the dashed horizontal line. The high proportion of orientation-tuned cells suggests that the response is not merely caused by the simultaneous presentation of two disparities but depends also on their spatial arrangement.

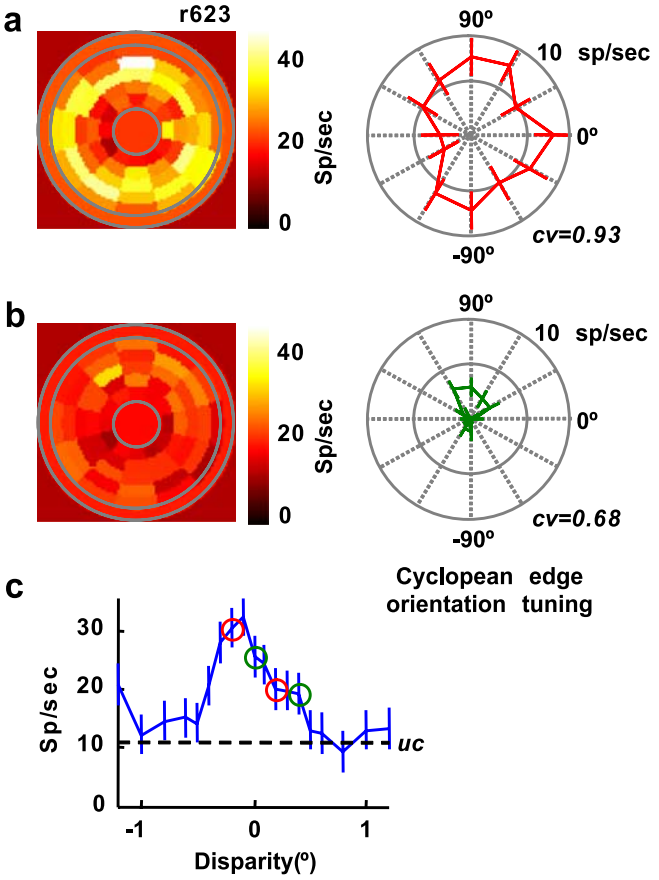

Figure 8. Example of a response that is selective for cyclopean edges but not for their orientation. ***a***, ***b***, Plotting conventions for the pseudocolor and polar plots are the same as in Figure 6, *a* (pseudocolor plot) and *c* (polar plot), except that there is no vector average shown in the polar plots (because of the absence of a defined preferred orientation). The examples in ***a*** and ***b*** were measured using different disparity pairs in the same neuron. ***c***, Disparity tuning curve for this example neuron. The dashed line indicates the response to uncorrelated dots. The disparities used to define the edge in ***a*** and ***b*** are shown in red and green dots, respectively. Although the disparities used in both cases are similar, the response in ***a*** is significant for cyclopean edge response enhancement, whereas the response in ***b*** is not. Sp/sec, Spikes per second.

An important advantage of our data set, which includes both edge orientation and position tuning, is that it allows us to isolate the cyclopean edge response, separate from the effects of the component disparities. Thus, our measures of orientation selectivity can meaningfully be compared with measures for other stimuli in other brain areas. Overall, V2 neurons appear only moderately selective for the orientation of cyclopean edges; the median value for circular variance ($cv = 0.76$) is larger than reported for V1 neurons for luminance gratings [$cv = 0.61$ (Ringach et al., 2002)]. However, this comparison with orientation tuning in V1 must be interpreted carefully. To measure the orientation tuning specific to cyclopean edges, we subtracted the expected response of a V1-like binocular energy cell. If we measure orientation tuning without making this adjustment (simply by calculating the mean firing rate over edge position for each orientation), the uniform disparity response acts as a large baseline term, greatly reducing the apparent orientation selectivity of the response. Figure 9*b* compares these two measures of orientation selectivity. Almost all of the points fall considerably above the identity line, indicating that the baseline term, resulting from the response to uniform disparities, considerably increases the circular variance (median = 0.91). Thus, when comparing raw response rates, orientation selectivity for cyclopean edges in V2 is substantially poorer than orientation selectivity for luminance in V1. If subsequent processing extracts a signal that factors out responses to uniform disparity, the selectivity of the orientation signal for cyclopean edge would improve considerably, but it remains less strongly orientation selective, on average, than orientation signals for luminance in V1.

Circular variance alone gives an incomplete picture of the way in which cyclopean edge responses depend on edge orientation. To explore this more closely, we examined responses to cyclopean edges oriented orthogonal to the preferred orientation:

$$\text{Orthogonal index} = \frac{(r_{\theta_{\text{pref}+90}} + r_{\theta_{\text{pref}-90}})/2}{(r_{\theta_{\text{pref}}})},$$

where r_θ is the cyclopean edge response beyond that which can be explained by uniform disparity selectivity (see Materials and Methods). Because θ_{pref} generally took values that did not exactly correspond to the orientation of any of our stimuli, we calculated the orthogonal index (and the sign index described below) based on interpolated values of r_θ (see Materials and Methods). The mean value of the orthogonal index (Fig. 9*c*) in our population was 0.41, almost half the response to the preferred orientation. That this index was frequently substantial indicates that orientations orthogonal to the preferred frequently produced a cyclopean edge response (responses greater than can be explained by uniform disparity selectivity alone). The distribution of this index is continuous, indicating that responses intermediate between strongly orientation-selective responses (Fig. 6) and cyclopean enhancement to all edge orientations (Fig. 8) were common.

Similarly, the distinction between neurons that respond to both signs of disparity at the preferred orientation (Fig. 7) and those that respond to only one sign (Fig. 6) represent extremes of a continuum, with many cells showing unequal enhancement for opposite signs. We quantified this with the following sign index:

$$\text{Sign index} = \frac{r_{\theta_{\text{pref}+180}}}{r_{\theta_{\text{pref}}}},$$

which compares the cyclopean edge response at the preferred orientation and sign with that at the same orientation with the opposite disparity sign. More than half of the cells showed significant cyclopean edge responses for both signs of the preferred orientation of a cyclopean edge (46 of 65) (Fig. 9*c*, squares). For these cells, the response to the non-preferred sign was, on average, 71% as strong as the response to the preferred sign, although there was a significant fraction of cells that responded almost equally well to either sign (15 of 65 with a sign index of >0.9).

Together, these two indices capture how similar the activity of any one neuron is to the examples in Figures 6–8. Figure 9*c* shows a scatter plot of these two indices, with the locations of each example neuron marked. The broad scatter shows that the population contains many response patterns that are intermediate between the examples we have shown.

Figure 9c shows a correlation between the orthogonal index and the sign index ($r = 0.73$; $p < 0.001$). This correlation indicates that neurons showing cyclopean enhancement for edges of both disparity sign generally also show enhancement for orthogonal orientations. The relationship between the two indices suggests that cyclopean enhancement for both disparity signs partly reflects a reduced specificity for the spatial properties of the cyclopean edge, rather than a sophisticated representation of the edge independent of the sign of the edge. If the two indices were

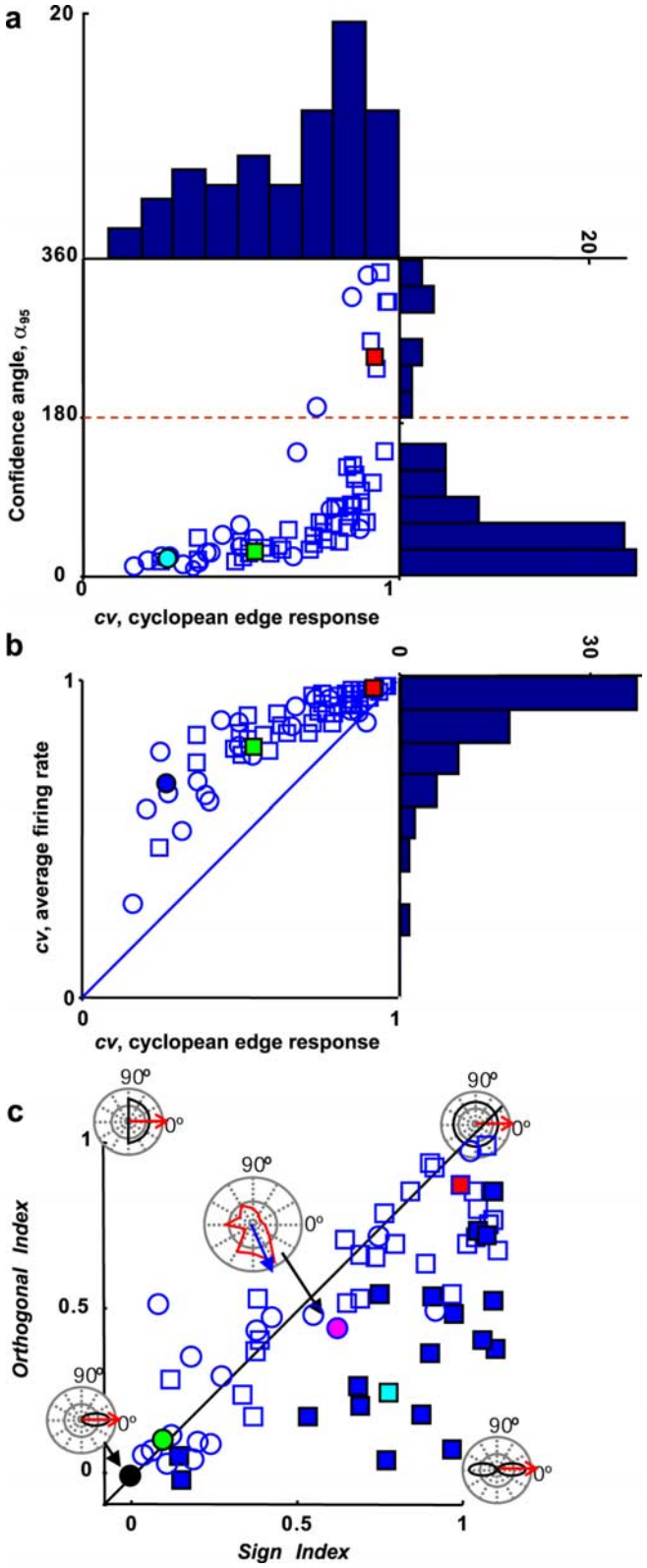

Figure 9. Population measures of orientation tuning for cyclopean edges. ***a***, Comparison of the circular variance with the confidence interval of the preferred orientation (α_{95}) for cyclopean edge-selective cells. Cells that responded significantly to both signs of a cyclopean edge are plotted as squares. The cyan, green, and red solid data points indicate the example responses in Figures 6–8, respectively (as they do in ***b*** and ***c***). The histogram projected above the scatter plot shows the distribution of the circular variance found in our sample. The histogram projected to the right of the scatter plot indicates the distribution of confidence angles in our data. The majority of cells are found below the horizontal line, indicating confidence angles of $<180°$ and reflecting significant orientation tuning. ***b***, Comparison of the circular variance calculated on the cyclopean edge response (*x*-axis) and on the average firing rate (*y*-axis). Almost all data points are located above the identity line, reflecting the large "baseline" component contributed by the response to uniform disparities, which does not change with orientation. ***c***, A more complete picture of the distribution of orientation-selective responses in the population is obtained by comparing the relative cyclopean edge responses for the non-preferred sign (sign index) and the orthogonal orientations (orthogonal index). Each index represents responses relative to the preferred orientation and sign. Points below the identity line responded better to the non-preferred sign of the preferred orientation than to orthogonal orientations (solid squares indicate data points in which this effect was significant). Note that both the orthogonal and sign indices can take negative values, indicating response suppression. The polar diagrams in each corner of the scatter plot represent idealized versions of the expected orientation tuning of a response falling in that quadrant. The solid pink data point is the response that was closest to the mean for both the sign and orthogonal indices. The orientation tuning of this example is shown in the central polar plot. cv, Circular variance.

scattered about the identity line, it would indicate that there was no real response enhancement to the non-preferred sign of the edge relative to non-preferred orientations; the tendency of the points to fall somewhat below the identity line ($p < 0.001$, paired *t* test) indicates that there is at least some specialization for the spatial properties of the edge, but this specialization is incomplete. It is notable that the data shown in Figure 7 is an extreme example, with exceptionally strong orientation tuning for both edge signs. A more typical example is shown in the polar plot at the center of Figure 9*c*, which is the data point that falls closest to the mean value for both indices. This example shows substantial cyclopean enhancement for all orientations, with the response at the preferred orientation but non-preferred sign slightly exceeding the response to orthogonal orientations.

The effect of edge location on responses to opposite edge signs

For cells that responded to both signs of a cyclopean edge, we asked whether this constitutes a representation of edge orientation that is invariant over the edge sign. This type of feature abstraction may be analogous to complex cells in V1, which respond to both signs of luminance contrast throughout their receptive fields. However, the analogy with complex cells in V1 breaks down when we consider the spatial distribution of the response to cyclopean edges of opposite sign. Two of the defining characteristics of complex cells are that they are selective for the orientation of a luminance edge regardless of the sign of the edge, and their response as a function of position does not depend on the sign of the edge. The example in Figure 7 shows that this pattern does not hold for cyclopean edge responses: although the response is orientation selective for both signs of a vertical edge, changing the sign of the disparity edge causes the cyclopean enhancement to occur for a different edge position. If this failure of position invariance is typical of the population results, it provides strong evidence against the case for feature abstraction in the cyclopean edge responses. Here, we examine how frequently responses to both signs of the cyclopean edge demonstrate position invariance.

We first selected cells that respond selectively to the orientation of edges of opposite signs. Of the 46 cells that responded significantly to both signs of the disparity edge, only 19 responded significantly better to both signs of the preferred orientation edge than they did to orthogonally oriented edges (Fig. 9*c*, solid data points). The remaining 27 cells responded as well or better to the orthogonal orientation as they did to the non-preferred sign of the preferred orientation (see the example data in Fig. 9*c*). The responses of these cells to the non-preferred edge sign are therefore not orientation selective. This alone establishes

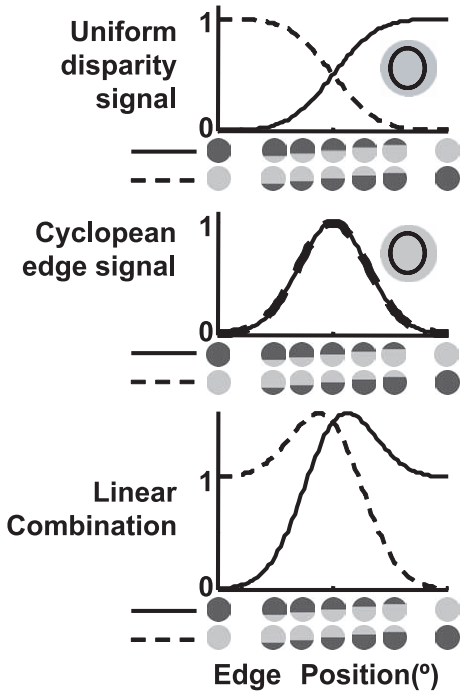

Figure 10. The influence of disparity signals and cyclopean edge responses on the location of response maxima. The neural response can be thought of as the combination of a uniform disparity signal (top) and a cyclopean edge signal (middle). Solid and dashed lines reflect responses to opposite sign edge stimuli. The idealized neuron responds in the same spatial location for both response components, as shown by the black oval superimposed on the gray stimulus icons. Summing the response components shown in the top and middle panels produces a response that peaks at different locations for opposite sign responses (bottom).

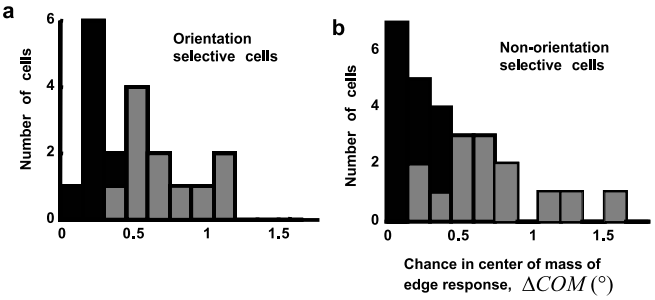

Figure 11. Effects of changes in edge sign on the location of cyclopean edge responses. The histograms plot the difference between the center of mass for cyclopean edge responses for opposite signs of the edge (at the preferred orientation). Only cells that showed a significant response to the non-preferred sign of an edge at the preferred orientation were included in this analysis. Gray bars indicate responses in which the center of mass of cyclopean enhancement was significantly different for opposite signs of the edge. ***a***, Cells with an orientation-selective response to both edge signs (respond better to both signs of an edge at the preferred orientation than they do to edges at orientations orthogonal to the preferred). ***b***, Cells only showing orientation-selective responses to the preferred edge sign (respond better or equally well to the orthogonal orientation as they do to the non-preferred sign of an edge at the preferred orientation).

that they do not represent edge orientation in a way that is invariant across sign.

Of the 19 cells that were orientation selective for both signs of the edge, we next asked whether the response was position invariant. In general, position invariance means that the neuron would have the same position tuning profile for both signs of an edge at a given orientation. However, the interpretation of position tuning curves is somewhat complicated for cyclopean edges because the response to changes in cyclopean edge location contains two components: a uniform disparity response and a cyclopean edge response. (Note that the analysis holds regardless of whether the two components represent different neural processes.) As illustrated in Figure 10, the combination of the two response components can cause the observed neural response to be maximal at different edge locations, even though the underlying spatial selectivity is identical. The top panel of Figure 10 shows a smooth transition between the responses to the component disparities. The solid and dashed lines represent the responses for opposite sign edges sweeping across the receptive field. The middle panel of Figure 10 illustrates the cyclopean edge response component, assuming the same underlying receptive field. The sum of these two response components peaks at different edge locations (Fig. 10, bottom panel), although the cyclopean component of the response is at the same location.

For this reason, we evaluated position invariance after subtracting the estimated contribution of a binocular energy cell (representing the uniform disparity response described above). This manipulation allows us to measure the location of maximum sensitivity for both signs of the cyclopean edge. We quantify the location preference by measuring the center of mass of the resulting cyclopean edge response (see Materials and Methods).

Figure 11 shows the results of this analysis for both orientation-selective and non-orientation-selective cells that respond to both signs of a cyclopean edge at the preferred orientation. More than 50% of cells show a significant difference in the center of mass (ΔCOM) for opposite sign edges regardless of their orientation selectivity (orientation selective, 11 of 19; non-orientation selective, 14 of 27). We also used the resample distributions to estimate the population distribution that would be expected from noise alone (see Materials and Methods). The observed differences are systematically greater than is expected from noise (Wilcoxon sign-rank test; orientation selective, $p < 0.001$; non-orientation selective, $p < 0.001$). There was no difference in these measures between orientation- and non-orientation-selective cells (Kolmogorov–Smirnov test, $p > 0.35$), suggesting that the cells in these groups are drawn from the same underlying distribution. This distribution does not seem to be consistent with the hypothesis of position-invariant contour detectors.

Despite the inherent difficulties with interpreting the peak locations of responses in raw data (as described in Fig. 10), we wanted to confirm that the lack of position invariance seen in the cyclopean edge responses is also apparent if we simply measure the change in location of the peak in the raw data. We found that the distribution of peak location differences ($\Delta\delta^{max}$) in the population (mean, 0.48°) was larger than expected by chance (based on the resample distributions; Wilcoxon sign test, $p < 0.001$). Individually, 6 of 19 cells responded maximally in different locations for opposite sign edges.

Finally, evaluating the raw data allows this question to be examined in a different way. Previous reports of cyclopean edge responses have compared responses to both signs of an edge in the same location and found that very few cells responded significantly to the non-preferred sign of the edge (von der Heydt et al., 2000; Qiu and von der Heydt, 2005). To confirm these results, we examined cyclopean edge responses when an edge of non-preferred sign is placed at the preferred orientation and location. Similar to previous results, we found that very few cells (9 of 46 cells with significant responses to both signs of the edge) responded significantly to this edge configuration.

The results for the majority of cells are similar to the pattern of responses that would be observed in V1 simple cells for opposite

sign luminance edges placed over an even-symmetric receptive field. Thus, in neurons that respond to both disparity signs of a cyclopean edge, the dependence on position and orientation suggest a simple-cell-like underlying receptive field structure (but in the disparity domain), rather than a generalization across disparity sign. That is, they resemble the responses of simple cells rather than complex cells to luminance.

Finally, we also looked at how selectivity for disparity compared with selectivity for cyclopean edge orientation. In particular, we wanted to know whether cells that were poorly tuned for disparity might be more likely to respond well to cyclopean edges. Such a trade-off might indicate that the binocular energy responses have already been factored out of the cyclopean edge response at the level of V2 cells. We measured the strength of disparity tuning using the disparity discrimination index (DDI) as described by Prince et al. (2002). We found no significant correlation between the *cv* and the DDI (data not shown). In addition, a *t* test comparing the DDIs of two groups of cells based on the significance of cyclopean edge selectivity found no significant difference. Thus, cyclopean edge selectivity is not confined to disparity-selective neurons. These results suggest that these responses are not merely a side effect of disparity selectivity, but represent some further specialization of disparity processing.

Generalization across disparities

We next examined the disparity dependence of cyclopean edge responses by testing edge responses using more than one pair of disparities in 28 neurons that responded significantly to cyclopean edges. This manipulation allowed us to differentiate between a disparity-invariant representation of edge orientation (a necessary requirement for cue invariance) and simple feedforward processing. If a simple mechanism based on feedforward input from a few disparity-selective neurons in V1 produces the cyclopean edge responses, we would expect small changes in the disparities used to define the edge to profoundly affect the response.

The most striking result was that most neurons only exhibited significant cyclopean enhancement for one disparity configuration (17 of 28). It is possible that some changes in disparity are more likely to abolish cyclopean edge responses than others (e.g., perhaps changes in the size of the disparity step are important, but not changes in the absolute disparity of the entire pattern). We examined both changes in the size of the disparity step and changes in the absolute disparity. We found that neither stimulus parameter had any predictive value in determining whether the neuron would respond significantly to a second stimulus configuration (median change in disparity step, 0.2°; median difference in absolute disparity, 0.2°). This pattern suggests that V2 cyclopean edge-specific cells are highly selective for the specific disparities used to define the edge. In one case, we even found significant response enhancement for edges defined by very different pairs of disparity values, but no response to a cyclopean edge defined with an intermediate disparity pair. These results support the idea of a receptive field that receives inputs from multiple V1 cells with different disparity preferences; responses of such a receptive field would tend to be very dependent on the specific disparities used.

Generalization across stimulus modality

Finally, we also considered whether cyclopean edge orientation tuning might be related to a general mechanism for identifying contour orientation across different stimulus modalities. We measured orientation selectivity for contrast-defined bars or gratings (whichever gave the best response) for 38 of the 65 cells that gave enhanced responses for cyclopean edges. We then compared the preferred orientation for both types of stimuli (Fig. 12*a*) for the 26 cells that were significantly orientation tuned for both modalities. We found that neurons with moderate to sharp orientation tuning for both types of stimuli ($cv < 0.75$; $n = 13$) (Fig. 12*a*, solid data points) revealed similar orientation preferences in both types of experiments, as indicated by the clustering of data points around the unit line ($p < 0.01$, permutation test). Figure 13*a* provides an example of a cell that was well tuned for both contrast and cyclopean edges. The preferred orientation for both types of stimuli is very similar. However, not all cells were equally well tuned for both contrast and cyclopean edges. The response shown in Figure 13*b* is well tuned for the orientation of a cyclopean edge but has a very broad response to a contrast stimulus, whereas the response in Figure 13*c* shows the opposite pattern. In both cases, the direction of the vector average for

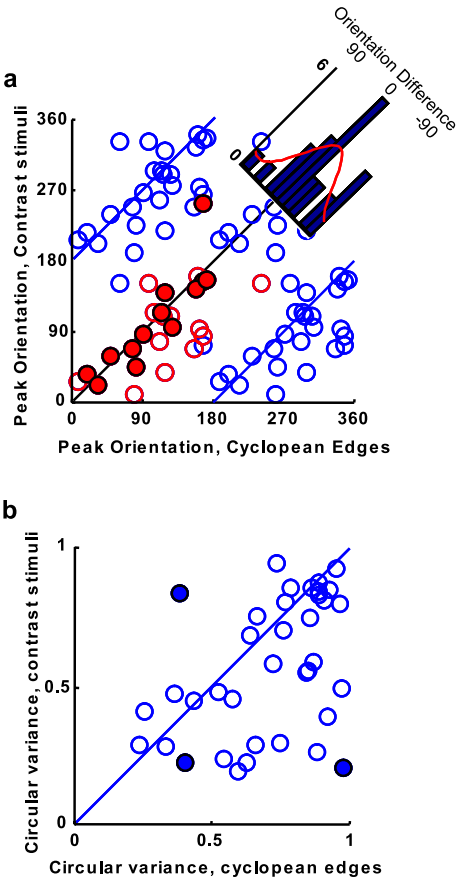

Figure 12. Comparison of orientation tuning for cyclopean edges and contrast-defined contours. ***a***, Preferred orientation for cyclopean versus contrast contours, for neurons showing significant orientation selectivity to both stimulus types. The solid lines indicate the identity line. To emphasize the circularity of the data (period of 180°), we plotted each data point four times, separated by 180° on the *x*- and *y*-axes. A single set of data points is plotted in red. Solid red symbols indicate cells in which the circular variance for both contrast stimuli and cyclopean edges was <0.75. Most of these neurons, for which preferred orientation is clear, lie close to the identity line, indicating similar orientation preferences for cyclopean edges and contrast stimuli. The histogram projected along the diagonal axis indicates the difference between the cyclopean edge and contrast orientation peaks for all cells that were jointly tuned for the orientation of contrast and cyclopean edges. The red line indicates the wrapped normal distribution that best approximates the data (SD = 41°). ***b***, Circular variance for cyclopean edges versus contrast stimuli. The diagonal line indicates the identity. Many neurons are considerably more selective for contrast stimuli than they are for cyclopean edges (indicated by points below the identity line; $p < 0.01$, paired *t* test). Solid symbols indicate example cells, shown in Figure 13.

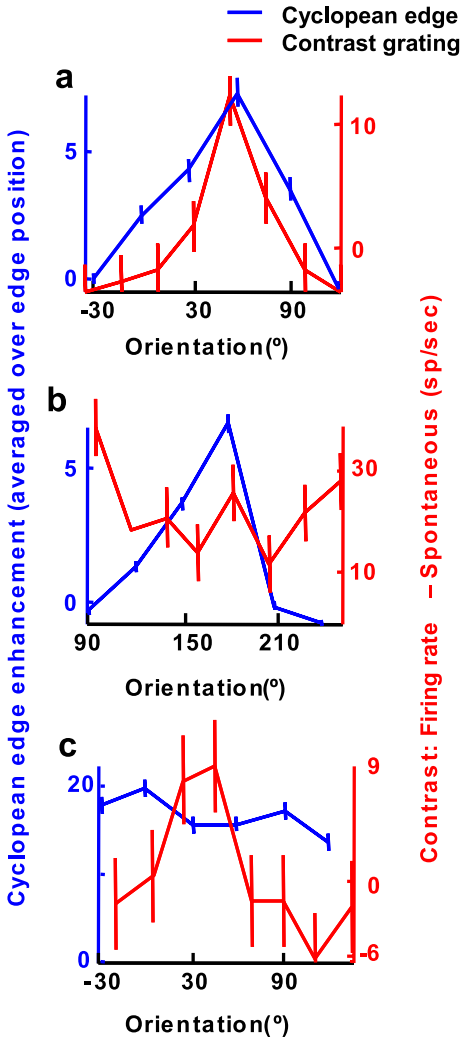

Figure 13. Examples of orientation tuning for cyclopean edges and contrast stimuli. Blue and red curves represent the responses to cyclopean edges and contrast stimuli, respectively. Note that the two curves have different axes: the axis for cyclopean edge stimuli is shown to the left of the data and indicates cyclopean edge response (see Materials and Methods), whereas the axis for contrast responses is shown to the right of the data and indicates the mean firing rate minus the spontaneous firing rate. Error bars indicate ±1 SEM (by resampling). ***a***, Cell that is well tuned for both types of stimuli. ***b***, Cell that is well tuned for cyclopean edges but not for contrast stimuli. ***c***, Cell that is well tuned for contrast but poorly tuned for cyclopean edges. sp/sec, Spikes per second.

contrast and cyclopean edges is very different, although there is a large overlap in the set of orientations that will produce a response. When cells were poorly tuned to either of these two stimuli ($cv > 0.75$), it was difficult to interpret any difference in preferred orientation. We found no cells that were sharply tuned to both stimuli, yet responded to very different orientations depending on the stimulus modality.

The correlation between peak orientation for contrast and cyclopean stimuli suggests that these cyclopean edge responses may reflect a specialization for cue-invariant contour representation. However, such a specialization should also produce similar magnitudes of orientation selectivity for different stimuli. The relationship between the circular variances for the different types of stimuli is shown in Figure 12*b*. We found that cells were frequently more sharply tuned for contrast than they were for cyclopean edges ($p < 0.01$, paired t test). Thus, although the correlation between preferred orientations does suggest some specialization for contour processing, the lack of correlation between circular variances indicates that any such specialization is incomplete.

Discussion

We measured responses of V2 neurons to single cyclopean edges (defined only by disparity in random dot patterns) for a wide range of orientations and edge positions. Previous studies demonstrating orientation selectivity for cyclopean edges in V2 have used stimuli in which the cyclopean edge forms part of a larger figure (von der Heydt et al., 2000; Qiu and von der Heydt, 2005). The presence of a figure in the stimuli used in these studies makes it difficult to determine whether cyclopean edge responses reflect a simple feedforward mechanism or whether they are part of a sophisticated representation of figure boundaries (von der Heydt et al., 2000; Qiu and von der Heydt, 2005). Although these studies recognized that cyclopean edge responses could be computed locally, their data did not allow this possibility to be tested directly.

Here, we used the most impoverished stimulus possible to define a cyclopean edge to evaluate the contribution of feedforward, local processing to cyclopean edge responses in V2. Because this stimulus contains no perceptual figure, the observed cyclopean edge responses cannot be explained by figure-ground interactions.

We found that a substantial fraction of neurons (65 of 139) significantly enhance their responses for a cyclopean edge beyond what could be produced by a simple disparity detector (i.e., a V1 cell), and, in most cases, this enhancement is orientation selective. The fact that our results mostly confirm those of von der Heydt et al. (2000) demonstrates that segmentation of the scene into figure and ground is not a necessary requirement for obtaining cyclopean enhancement: it seems that a suitable arrangement of stimulus disparities in the vicinity of the receptive field is sufficient.

In addition to confirming previous findings, our quantitative analysis reveals three important characteristics of cyclopean edge responses. (1) Because previous studies did not isolate the response component that was specific to cyclopean edges, they were unable to analyze orientation selectivity quantitatively (von der Heydt et al., 2000). Our analysis reveals that although significant orientation selectivity is common, it is rarely as strong as orientation selectivity (for luminance) in V1. (2) Responses to cyclopean edges depend strongly on the disparities used to define the edge: small changes in disparity can abolish the response to cyclopean edges. (3) Although approximately two-thirds of the neurons respond significantly to both edge signs, in many cases the preferred sign for an edge depends on edge location. Consequently, when tested at any one location, the response may appear to be sign specific, as reported previously (von der Heydt et al., 2000; Qiu and von der Heydt, 2005).

Points 2 and 3 represent a failure to signal edge orientation in a way that is invariant across disparity. Point 2 is particularly damaging because it means that the detection of edges in these cells will not survive changes in vergence angle. Point 3 also represents a dependence on disparity, because opposite edge signs differ only in disparity. At first sight, responses to both edge signs appear to be a useful generalization across disparity. However, we show that the location at which a response is elicited changes substantially with edge sign. The interdependence of edge loca-

tion and disparity sign is therefore a failure to signal edge orientation in a way that is cue invariant.

In considering the overall degree of cue invariance that V2 cells show for cyclopean contours, the responses of V1 complex cells to luminance are a useful reference. The orientation selectivity of V1 complex cells does not depend on luminance or contrast sign. In contrast, cyclopean edge responses in V2 are strongly dependent on disparity, demonstrating less complete cue invariance than is found in V1 (for luminance).

Our results suggest that a simple feedforward mechanism pooling inputs from V1 subunits with different receptive field locations and disparity tuning may be sufficient to explain cyclopean edge responses in macaque V2. Because the converging inputs have different disparity preferences, the receptive field would respond best when each subfield is stimulated by its own preferred disparity. Such a mechanism is closely analogous to the way feedforward models of V1 suggest that simple cells pool inputs from lateral geniculate nucleus neurons with different receptive field locations and different luminance preferences (i.e., "on" or "off" center cells) (Hubel and Wiesel, 1962; Reid and Alonso, 1995; Ringach, 2004; for review, see Ferster and Miller, 2000).

In the simplest feedforward model that could explain our results, V2 cells would receive input from just two V1 subunits with different disparity preferences. At least two properties of such a scheme are evident without implementing a specific model. (1) Neurons should respond more strongly to the optimal cyclopean edge than to any stimulus of uniform disparity. This prediction reflects the fact that, if the subunits are tuned to different disparities, no uniform disparity can optimally activate both subunits. (2) Cyclopean enhancement only occurs when the subunits have different responses to the disparities used to define an edge. Consequently, cyclopean edge responses should depend critically on the specific disparities used to define the edge stimulus. These predictions are consistent with the results described here.

Even if pairs of V1 inputs were chosen at random, many such pairings would generate cyclopean enhancement for an edge defined by the appropriate disparities. It is therefore possible that a random convergence from V1 to V2 might explain the data discussed so far. However, one result reported by von der Heydt et al. (2000), which we replicated with our impoverished stimulus, cannot be explained by such random pairings: the preferred orientation for cyclopean edges tends to be similar to that for contrast-defined contours. Although it is not difficult to produce this in a simple feedforward scheme, it does require an appropriate relationship between the receptive field positions of the subunits and their preferred orientations. These data demonstrate a form of cue invariance that goes beyond what is available in V1. This represents a useful step toward a sophisticated contour representation, even if it can be explained by simple mechanisms.

However, very simple schemes, such as the one we propose here [also considered by von der Heydt et al. (2000)], produce more limited cue invariance than has been proposed previously, and these limitations are demonstrated by our observations. Importantly, several failures of cue invariance became apparent only when responses were examined over a wide range of edge orientations and positions. This has significant implications for studies that limit their analyses to a single contour location. For example, Qiu and von der Heydt (2005) reported that some neurons that responded to a luminance-defined "figure" on one side of the receptive field also tended to respond to a figure defined solely by near disparities at the same location. The congruence of the "foreground" signal for luminance with the near disparity signals suggest a high-level encoding of figure-ground segregation. Our results indicate that this finding may depend critically on the location at which the comparison is made.

It is important to stress that our results were all obtained with an impoverished stimulus, containing only a single edge. It is possible that a different set of results would be obtained if a disparity-defined figure, such as that used previously (von der Heydt et al., 2000; Qiu and von der Heydt, 2005), was used. We also cannot rule out the possibility that our impoverished stimulus may only stimulate a subset of the neurons identified by von der Heydt and colleagues (von der Heydt et al., 2000; Qiu and von der Heydt, 2005). Thus, our data in no way contradict previous observations, although they do raise the possibility of a simple, feedforward explanation.

The idea that V1 cells with different tuning characteristics may be combined in V2 to produce more sophisticated signals has been suggested previously to explain other properties of V2 neurons. Ito and Komatsu (2004) suggested such a scheme to explain responses to angle stimuli, an idea developed further by Boynton and Hegde (2004). Similarly, Hegde and Van Essen (2000) invoked the idea of convergence from V1 onto V2 cells to account for selectivity for complex contours. Similar schemes may also explain responses to motion borders (Marcar et al., 2000), illusory contours (von der Heydt et al., 1984, 1992), and relative disparity (Thomas et al., 2002).

The detailed characterization of cyclopean edge responses presented here is compatible with this feedforward explanation and provides a rich data set with which to test such simple schemes. In addition, several features of the results indicate a failure to produce a disparity-invariant representation of edge orientation. Together, this argues that, although processing in V2 is more sophisticated than processing in V1, V2 cyclopean edge responses represent an incomplete specialization for figure/ground segmentation. Rather, they perform many of the initial computations required to support such processing further up the pathway.

References

Adelson EH, Bergen JR (1985) Spatiotemporal energy models for the perception of motion. J Opt Soc Am A 2:284–299.

Boynton GM, Hegde J (2004) Visual cortex: the continuing puzzle of area V2. Curr Biol 14:R523–R524.

Ferster D, Miller KD (2000) Neural mechanisms of orientation selectivity in the visual cortex. Annu Rev Neurosci 23:441–471.

Fleet DJ, Wagner H, Heeger DJ (1996) Neural encoding of binocular disparity: energy models, position shifts and phase shifts. Vision Res 36:1839–1857.

Hawken MJ, Shapley RM, Grosof DH (1996) Temporal-frequency selectivity in monkey visual cortex. Vis Neurosci 13:477–492.

Hegde J, Van Essen DC (2000) Selectivity for complex shapes in primate visual area V2. J Neurosci 20:RC61(1–6).

Hubel DH, Wiesel TN (1962) Receptive fields, binocular interaction and functional architecture in the cat's visual cortex. J Physiol (Lond) 160:106–154.

Ito M, Komatsu H (2004) Representation of angles embedded within contour stimuli in area V2 of macaque monkeys. J Neurosci 24:3313–3324.

Leventhal AG, Wang Y, Schmolesky MT, Zhou Y (1998) Neural correlates of boundary perception. Vis Neurosci 15:1107–1118.

Marcar VL, Raiguel SE, Xiao D, Orban GA (2000) Processing of kinetically defined boundaries in areas V1 and V2 of the macaque monkey. J Neurophysiol 84:2786–2798.

Mardia KV, Jupp PE (2000) Directional statistics. Chichester, UK: Wiley.

Moore IV BD, Alitto HJ, Usrey WM (2005) Orientation tuning, but not direction selectivity, is invariant to temporal frequency in primary visual cortex. J Neurophysiol 94:1336–1345.

Ohzawa I (1998) Mechanisms of stereoscopic vision: the disparity energy model. Curr Opin Neurobiol 8:509–515.
Ohzawa I, DeAngelis GC, Freeman RD (1990) Stereoscopic depth discrimination in the visual cortex: neurons ideally suited as disparity detectors. Science 249:1037–1041.
Prince SJ, Pointon AD, Cumming BG, Parker AJ (2002) Quantitative analysis of the responses of V1 neurons to horizontal disparity in dynamic random-dot stereograms. J Neurophysiol 87:191–208.
Qiu FT, von der Heydt R (2005) Figure and ground in the visual cortex: V2 combines stereoscopic cues with gestalt rules. Neuron 47:155–166.
Read JC, Cumming BG (2003) Measuring V1 receptive fields despite eye movements in awake monkeys. J Neurophysiol 90:946–960.
Reid RC, Alonso JM (1995) Specificity of monosynaptic connections from thalamus to visual cortex. Nature 378:281–284.
Ringach DL (2004) Haphazard wiring of simple receptive fields and orientation columns in visual cortex. J Neurophysiol 92:468–476.
Ringach DL, Shapley RM, Hawken MJ (2002) Orientation selectivity in macaque V1: diversity and laminar dependence. J Neurosci 22:5639–5651.
Thomas OM, Cumming BG, Parker AJ (2002) A specialization for relative disparity in V2. Nat Neurosci 5:472–478.
von der Heydt R, Peterhans E, Baumgartner G (1984) Illusory contours and cortical neuron responses. Science 224:1260–1262.
von der Heydt R, Peterhans E, Dursteler MR (1992) Periodic-pattern-selective cells in monkey visual cortex. J Neurosci 12:1416–1434.
von der Heydt R, Zhou H, Friedman HS (2000) Representation of stereoscopic edges in monkey visual cortex. Vision Res 40:1955–1967.
Zhou H, Friedman HS, von der Heydt R (2000) Coding of border ownership in monkey visual cortex. J Neurosci 20:6594–6611.